CFD SIMULATIONS TO PREDICT THE ENERGY EFFICIENCY OF AN AXIAL FAN FOR VARIOUS CASING CONFIGURATIONS

Alain GUEDEL[1], Mirela ROBITU[1], Vivian CHAULET[2]

[1] *CETIAT, 25 avenue des Arts, B.P. 2042, 69100 Villeurbanne cedex, France*

[2] *Ziehl-Abegg FMV, Rue de la Gare, 01800 Villieu, France*

ABSTRACT

The objective of this paper is to compare the measured and predicted performances of a tubeaxial fan for different casing configurations. This work is motivated by the European regulation with regard to ecodesign requirements for fans driven by electric motors. The prediction is made with the CFD commercial code STAR-CCM+. The agreement between the experimental and numerical results on fan efficiency is very satisfactory.

INTRODUCTION

The implementation of the Energy Related Products Regulation applied to fans (ErP lot 11) fixes minimum energy efficiency requirements for fans from 1 January 2013 [1]. The target energy efficiency is based on the electrical input power of the motor at the best efficiency point of the fan, the efficiency being total or static according to the installation category A, B, C or D.

The minimum efficiency levels imposed by the regulation may sometimes be difficult to achieve, which forces the fan manufacturers to improve the efficiency of their products by choosing an efficient motor and optimizing the geometry of the impeller and casing as well as their respective location in the fan.

The evaluation of the performance of various fan configurations by tests on mock-ups that have to be built up is quiet expensive. Flow simulations may prove quite interesting to perform a parametric study in order to predict the performance of various fan configurations once they have been validated on a reference case by comparison with experiment. The cost of simulations may indeed be lower than the experiments.

To help the manufacturers in this task, the objective of this work is to assess the ability of a method of simulation of axial flow fans to predict the impeller efficiency with a reasonable accuracy using three-dimensional CFD models. The study has been carried out on a low-pressure axial fan of 630 mm diameter with four different casing configurations. Measurements of the fan performance

have been carried out by Ziehl-Abegg FMV on the different setups and the test data have been compared to results of simulations performed by CETIAT.

The first part of the paper presents the experimental configuration describing the fan, the casing geometry and the measurement setup as well as the test method. The second part describes the numerical model, the last part presents the comparison of the measured and predicted performance data with an analysis of the results.

TEST SETUP AND EXPERIMENTAL RESULTS

Fan and casing configurations

The fan selected for this study is a tubeaxial fan (see Figure 1) with the following geometry:

- impeller diameter: 624 mm
- number of blades: 12
- hub/tip ratio: 0.34
- blade pitch angle at the hub: 30°
- tip chord length: 64 mm
- average tip clearance: 3 mm
- rotation speed: ≈ 1440 rpm

The electric motor is a three phase AC motor with 4 poles, placed downstream of the impeller. The motor support is non axisymmetric as shown in Figure 1.

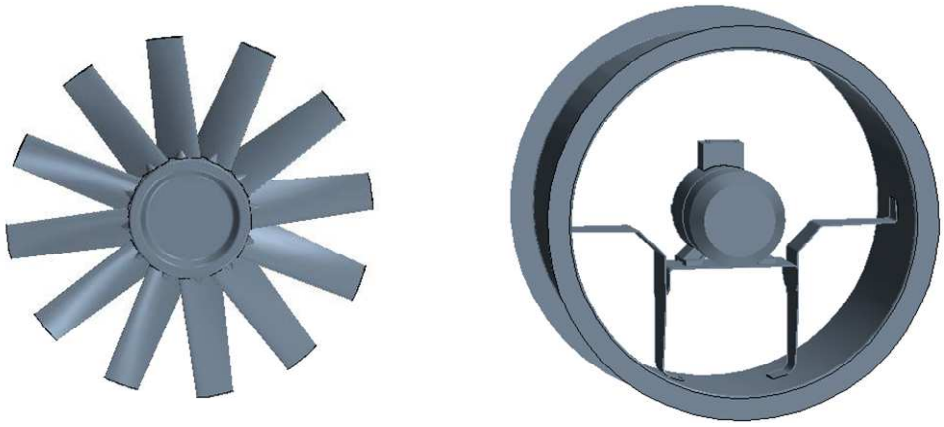

Figure 1 Impeller and casing with the motor and its support

Four configurations of casings of 630 mm internal diameter have been tested and simulated to quantify their influence on the fan performance. The characteristics of the casings are respectively:

- long casing with inlet bellmouth (Figure 2(a))
- long casing without inlet bellmouth (Figure 2(b))
- short casing with inlet bellmouth (Figure 2(c))
- long casing + inlet duct of 1L length with inlet bellmouth + outlet duct of 2L length, where L is the casing length (Figure 2(d)).

The first three fan configurations are tested according to installation category A (free inlet, free outlet), while the fourth setup simulates installation category D (ducted inlet, ducted outlet).

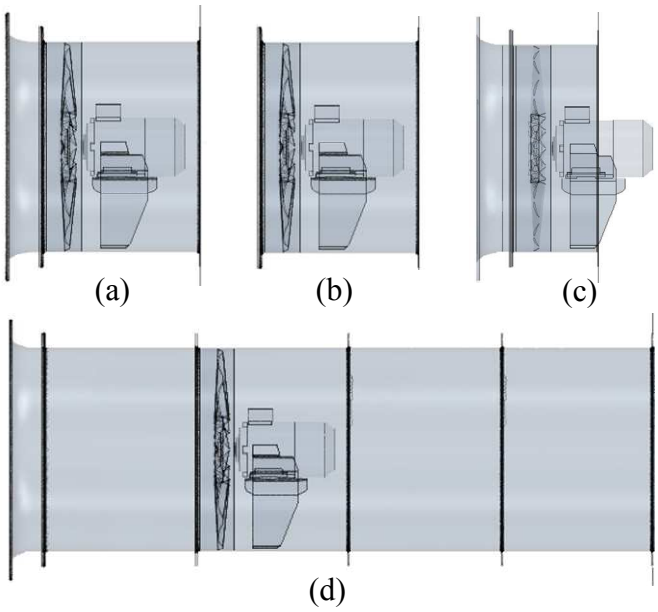

Figure 2 Configurations of casing tested

Test facility and measurement method

The fan tests have been performed by Ziehl-Abegg FMV on their test rig which is an outlet test chamber with a cross section area equal to 17 times the duct cross section of the fan (Figure 3).

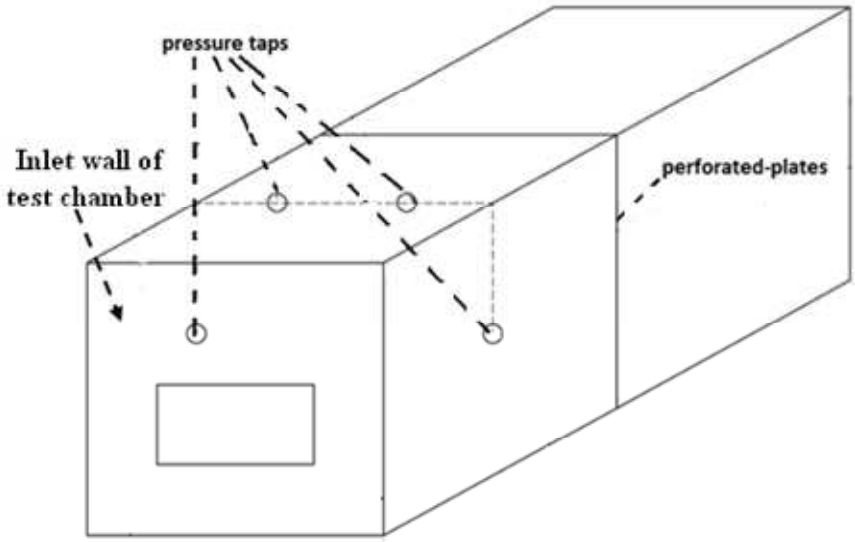

Figure 3 Fan test rig

The outlet chamber comprises perforated-plate screens in the middle section of the chamber to homogenize the flow. Four static pressure taps are located in a plane at a distance of 0.26 L_0 from the inlet wall, where L_0 is the length of the test chamber.

The fan is mounted on the inlet wall of the chamber and an auxiliary fan with variable speed, placed in the chamber downstream of the perforated plates, is used to control the fan operating point. The

flowrate of the fan is determined outside of the chamber with an orifice plate at the end of the outlet duct of the auxiliary fan, while the fan pressure is obtained from the measurements with the four pressure taps. The fan speed and the input power of the electric motor are measured simultaneously with the flow and the pressure of the fan at each operating point. Both the test rig and the measurement method are in conformity with ISO 5801 [2].

Experimental results

The test data obtained for a rotation speed N ≈ 1440 rpm have been converted to reference conditions N_0 = 1445 rpm, ρ_0 = 1.2 kg/m³. Figure 4 (a) shows the measured fan static pressure curves for the four casing configurations tested. Figure 4 (b) shows the measured overall efficiency curves with the different casings, the overall efficiency being the ratio of the fan static power (volume flow rate multiplied by static pressure) divided by the motor input power. Some differences are observed between the static pressure curves as well as between the efficiency curves, the best performance being obtained with the long casing – installation category D while the worst performance at the peak static efficiency is measured with the short casing with bellmouth. At the peak efficiency (near 7500 m³/h) the difference in static pressure is about 30 Pa and the difference in static efficiency attains 5.5% between these two configurations.

The comparison of the measured and predicted performances of the four casing configurations will be made at several flow rates between 6000 m³/h and 10000 m³/h, i.e. in an acceptable flow range for fan operation. Indeed, in an informative annex of ISO 12759 [3] a recommendation is made to save energy which specifies that a fan should operate in a flow range where the efficiency is not less than 85% of its peak efficiency.

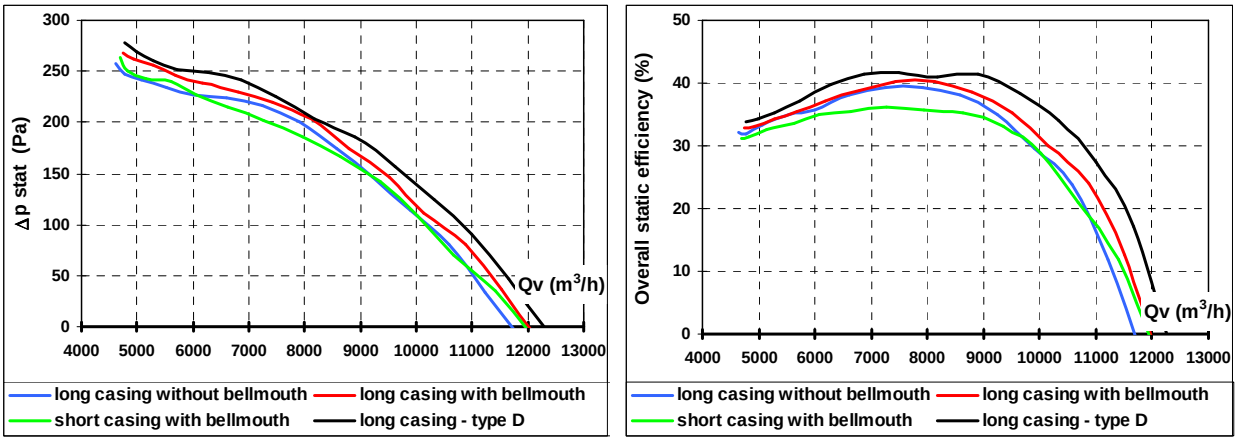

(a) (b)

Figure 4 (a) Measured static pressure curves, (b) Measured overall static efficiency curves

CFD SIMULATIONS

A stationary three-dimensional CFD modeling of the fan mounted in the test facility is conducted in order to simulate the axial flow fan. The commercial code STAR-CCM+ version 6.02.009 was used in this study.

Firstly, the cleaning up of the CAD geometry provided by the fan manufacturer and the calculation domain conception are carried out. The outlet test chamber of the computational domain strictly reproduces the experimental setup with its actual dimensions.

Then, the surface mesh of calculation domain is generated with progressive element size. Due to the complexity of the blade geometry, an unstructured polyhedral volume mesh is generated. The mesh features a refined mesh close to the fan in order to capture the flow variation due to the presence of the solid elements, including a boundary-layer grid near the blade surface (see Figure 5 (a)), and a coarser mesh towards the ends of the calculation domain (see Figure 5 (b)). The final volume mesh grid of the calculation domain consists of 14,656,000 elements.

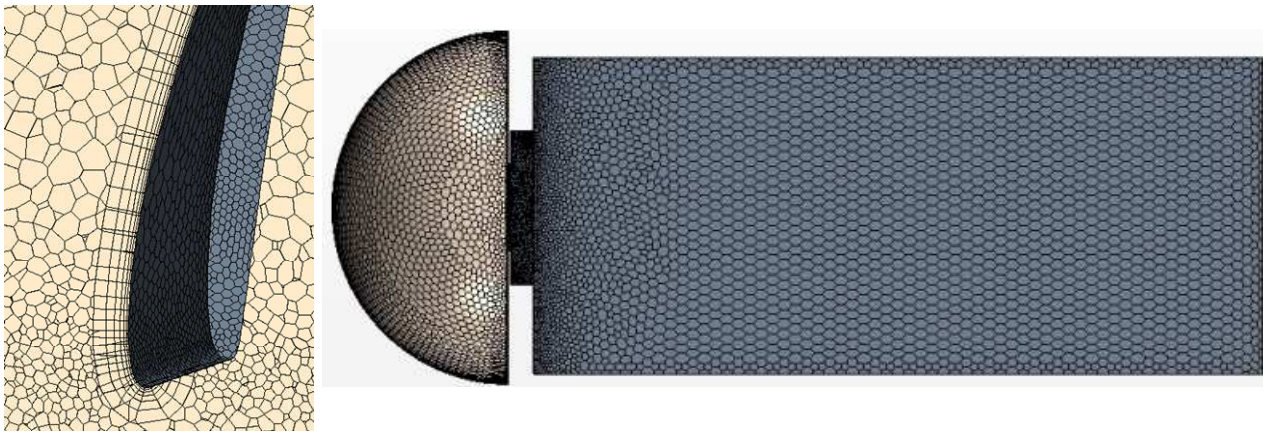

(a) (b)

Figure 5: Calculation domain mesh (a) zoom of the mesh in the blade area, (b) volume mesh

The fan in its test facility is modeled with the multiple reference frame method (MRF). The fluid region in the fan area is modeled in a rotating reference frame. Fluid surrounding the fan area is modeled in a stationary frame (see Figure 6).

The steady Navier–Stokes equations with realizable two-layer k–ε turbulence model including all y+ wall treatment are used. To simulate this model a second order upwind differencing scheme is used. To check the model convergence, in addition to the default residuals a surface monitor is set at the inlet MRF region to monitor the mass flow rate and the pressure. The stabilization of the mass flow rate and pressure provides an indication of the physical solution convergence.

Computational grid and boundary conditions

The boundary conditions for computation domain are illustrated in Figure 6. The computation domain is divided in two regions. The first region corresponds to the main flow outside the fan, a stationary region that consists of 7,092,284 volume elements. The second region corresponds to the fluid near the fan (MRF region) and consists of 7,564,342 volume elements. The MRF region includes the rotating parts (blades and hub). The circumferential limit of the MRF region is in the tip clearance at approximately half-distance between the blade tip and the casing. The Inlet boundary condition is “Stagnation Inlet” with total pressure equal to zero and the Outlet boundary is “Mass Flow Outlet” imposed. The fan walls are modeled as rotational moving walls with zero velocity relative to the adjacent cell zone. The other walls of the domain are modeled as stationary walls. The inlet turbulent intensity and turbulent length scale were chosen constant and equal to 0.1 and 0.01m respectively. Initial field values within the computation domain are chosen to hasten convergence. The flow field is simulated on the whole impeller (i.e. no periodicity conditions are assumed) and the calculation is done on the total actual domain. The simulations are made for at least three flow rates per configuration: 7416, 8700 and 10008 m³/h. The fluid in the MRF region is rotating at 1445 rpm. The simulations were realized on two workstations, XEON 2.93 GHz, 128 GB RAM, with 22 parallel processors and took 15 hours minimum per fan operating point.

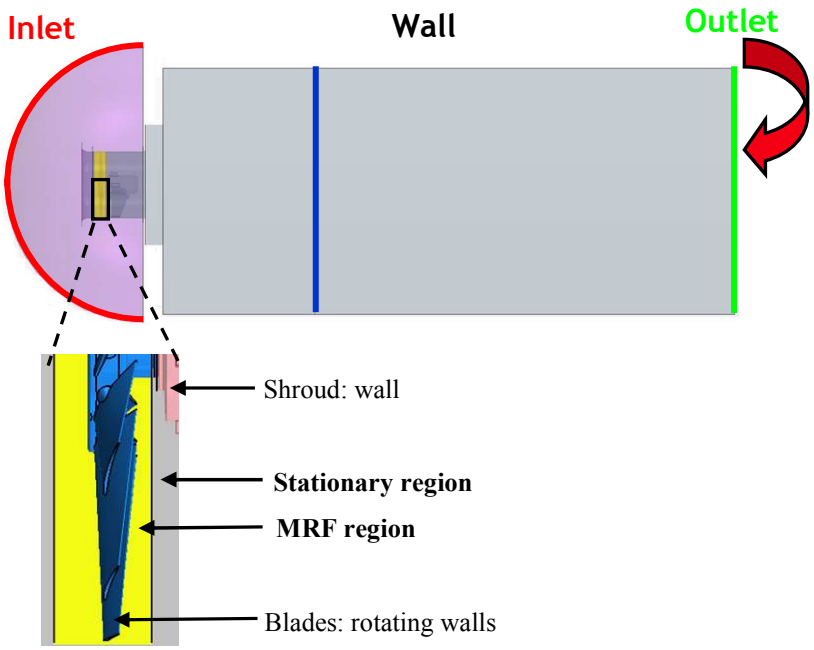

Figure 6: Boundary conditions of the calculation domain

For each simulation case the average static pressures at the inlet of the computational domain and in the section of the pressure taps are recovered and the fan static pressure is deduced. The torque on the propeller is also recovered to obtain the motor input power.

Simulations results

Figure 7 shows the contours of velocity magnitude in the horizontal midplane for the "long casing with bellmouth, installation category A" and two flow rates, 7416 m³/h and 10008 m³/h. The flow velocity downstream the fan is slightly radial for the low flow rate (Figure 7 (a)) and axial for the large flow rate (Figure 7 (b)).

Figure 8 shows the contours of velocity magnitude in the horizontal midplane for the "long casing, installation category D" at 7416 m³/h only. In this case, the flow is more axial than with installation category A in Figure 7 (a).

In Figures 7 and 8 the flow velocity pattern in the horizontal plane is not symmetrical with respect to the fan axis. This is mostly due to the presence of the motor support that constitutes a non-symmetric obstruction to the swirl flow at the impeller exit.

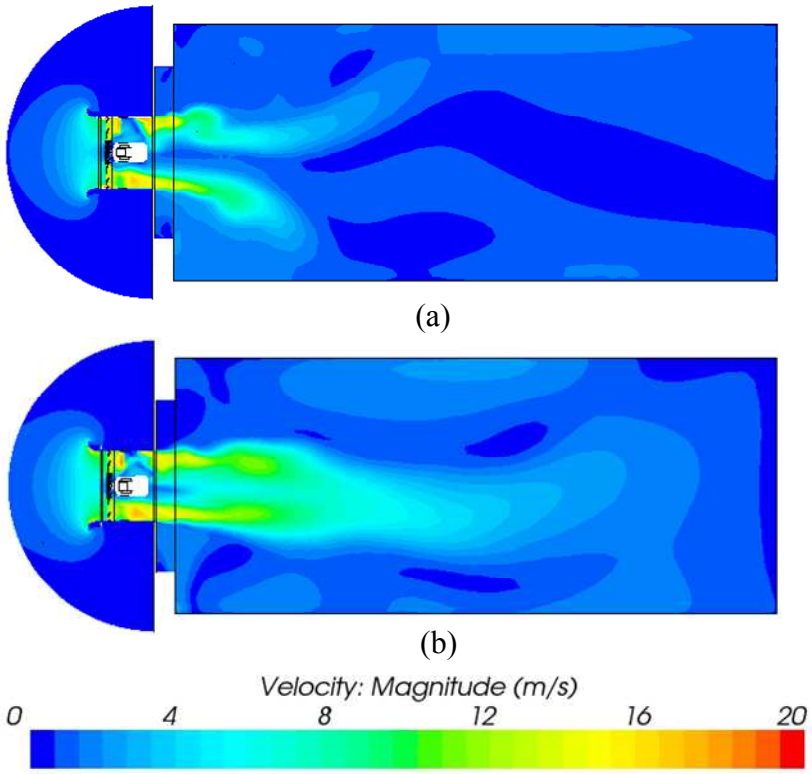

Figure 7 Contour of velocity magnitude in the horizontal midplane for the case "long casing with bellmouth, installation category A" (a) Qv = 7416 m³/h, (b) Qv = 10008 m³/h

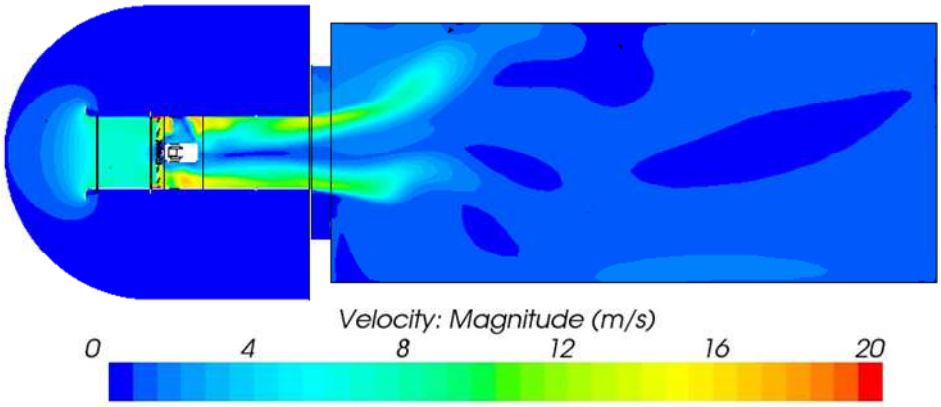

Figure 8: Contour of velocity magnitude in the horizontal midplane for the case "long casing, installation category D", Qv = 7416 m³/h

VALIDATION OF THE CFD MODEL

In a previous stage, CFD simulations were carried out to compare fan pressure results obtained by imposing the mass flow rate at the inlet and at the outlet of the calculation domain. This comparison highlighted that imposing the mass flow at the outlet led to results closer to the experiment than when the flow was imposed at the inlet. For this reason, the results presented hereafter are obtained by imposing the mass flow rate at the outlet of the calculation domain.

Figure 9 compares the measured and predicted fan performance data for the long casing with inlet bellmouth, installation category A, at four flow rates. This figure shows the curves of static pressure, motor input power and overall static efficiency respectively.

The predicted motor input power is determined from the calculated impeller power $Pr = C.\omega$, where C is the calculated torque in N.m and $\omega = 2\pi N$ is the rotation speed in rad/sec, and the motor efficiency, which is constant and equal to 75 % in the torque range considered.

Figure 9 shows the influence of the number of computational iterations on the prediction: simulation 1 shows results obtained after about 2000 iterations (12 to 15h cpu time) while in simulation 2 the number of iterations exceeds 20 000 (≈ 70h cpu time).

These results show a good agreement between the experiment and the prediction with many iterations (simulation 2) for all the calculated flow rates and the three series of curves. The agreement is less good on the static pressure and input power curves with less iterations (simulation 1) at the two lower flow rates because the calculation has not yet fully converged (see discussion later on). The predicted values of overall static efficiency are close to the experiment with both simulations whatever the flow rate. For this reason the measured and predicted results of the other casing configurations will be presented with the large number of iterations only.

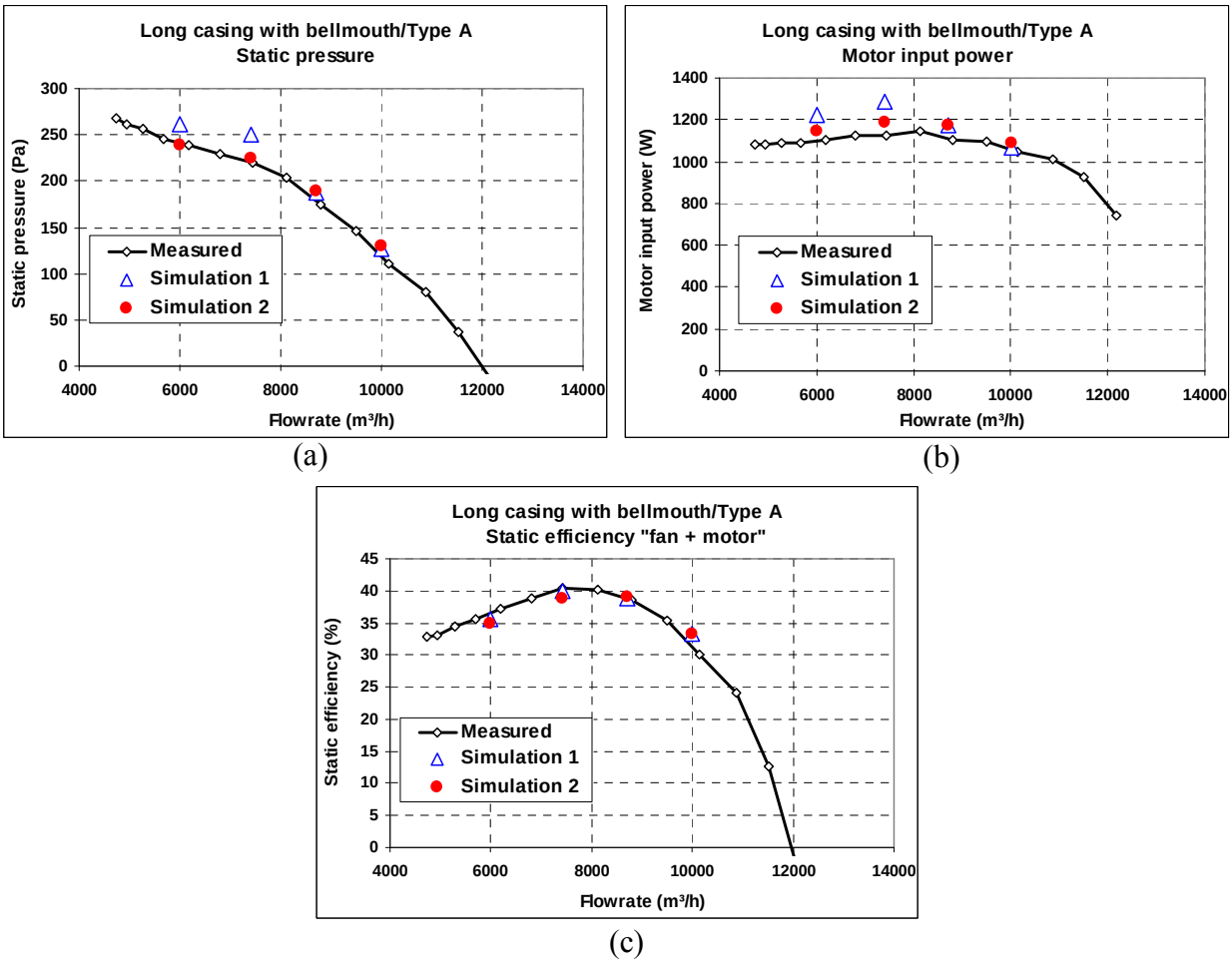

Figure 9 Comparison of measured and predicted results – Long casing with bellmouth: a) Static pressure, b) Motor input power, c) Overall static efficiency (simulation 1: ≈ 2000 iterations; simulation 2: ≈ 20000 iterations)

Figure 10 to Figure 12 compare measured and predicted results obtained for the three other casing configurations: long casing without inlet bellmouth, long casing type D and short casing with inlet bellmouth respectively. In these figures only the static pressure and the overall static efficiency are presented. For the cases with bellmouth (Figures 11 and 12) the prediction is very close to the experiment like in Figure 9 with many iterations (simulation 2). Conversely, for the case without bellmouth (Figure 10), the prediction is below the experiment on both static pressure curve and efficiency curve at peak efficiency. A possible explanation of this slight disagreement is proposed in the discussion below.

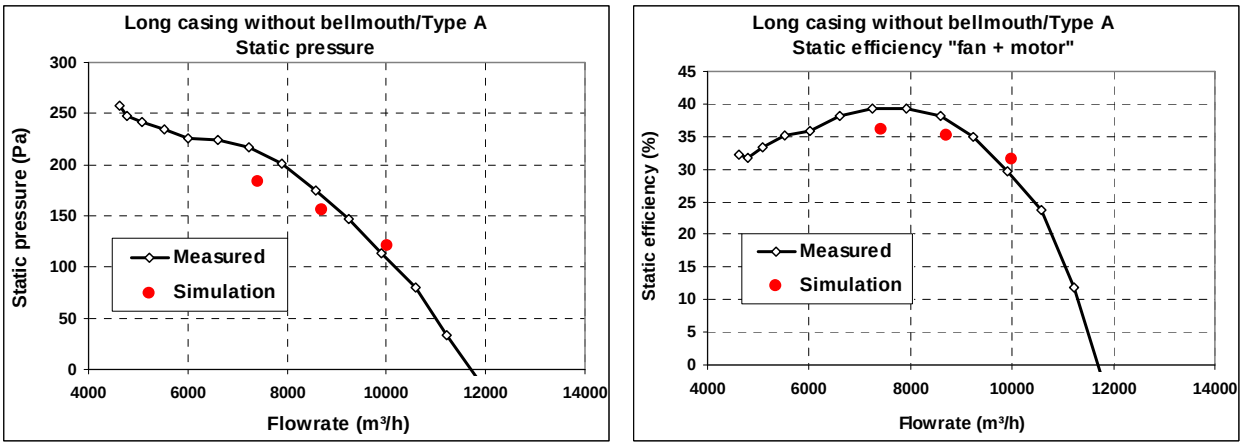

(a) (b)

Figure 10 Comparison of measured and predicted results – Long casing without bellmouth
(a) Static pressure, (b) Overall static efficiency

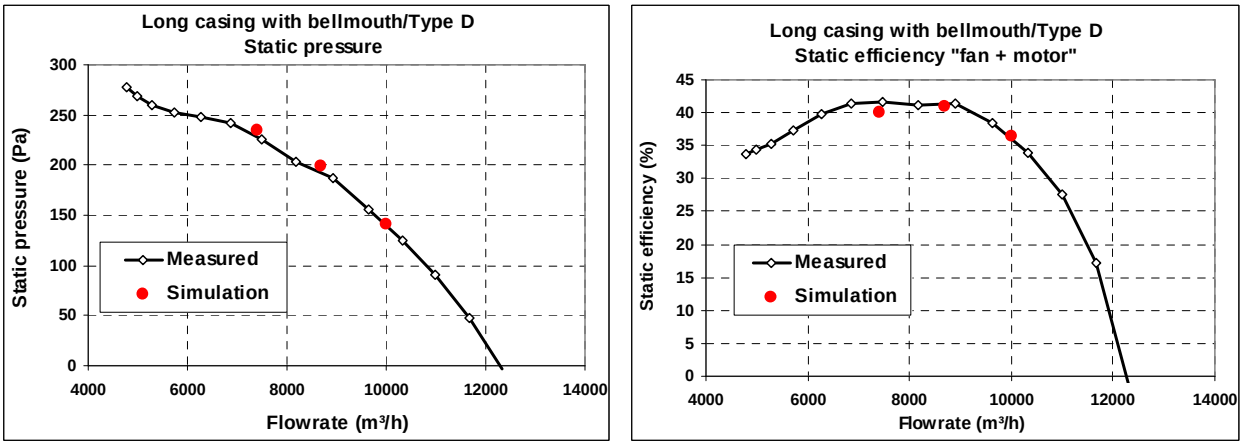

(a) (b)

Figure 11 Comparison of measured and predicted results – Long casing, installation category D
(a) Static pressure, (b) Overall static efficiency

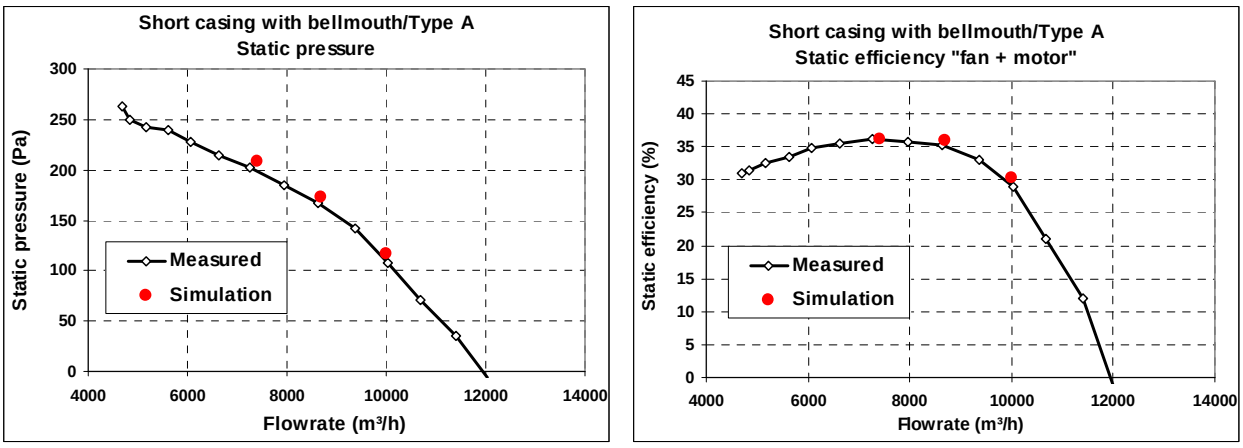

(a) (b)

Figure 12 Comparison of measured and predicted results – Short casing with bellmouth
(a) Static pressure, (b) Overall static efficiency

DISCUSSION AND CONCLUSIONS

The objective of the present study was to assess the ability of a CFD method based on steady RANS simulations to predict the fan efficiency with reasonable accuracy. The results presented in this paper prove that this objective is fulfilled since the prediction is globally quite close to the experiment, either for the static pressure curve or the overall efficiency curve, provided the number of iterations is sufficient to obtain physical converged solutions of the calculations. This study has shown that the cpu time needed to reach the convergence strongly depends on the fan operating point.

At high flow rate, i.e. well above the flow at the peak static efficiency, the calculations converge much quickly than at lower flow rate. This feature, which has been observed whatever the fan casing configuration, might be due to flow instabilities at low flow rate which could induce fluctuations of the numerical results and therefore would require a longer time to reach a stabilized solution. That may happen even at the peak static efficiency point, which is on the left side of the fan performance curve with respect to the best efficiency point based on the fan total pressure.

The difference between the predicted and experimental results is larger for the case without inlet bellmouth than for the three other cases. The absence of bellmouth may induce flow separation and instabilities in the fan that could partly explain this difference. Another complementary explanation of this gap could be due to the lack of mesh refinement in the stationary region close to the casing inlet which does not allow to capture the actual flow details with enough accuracy.

In conclusion, the prediction of the fan pressure and fan efficiency curves is considered as excellent for three of the four casing configurations tested. It is slightly less good for the configuration without inlet bellmouth for the reasons mentioned above. A careful watch of the physical convergence of the calculations is necessary to avoid erroneous results.

Further work on the same fan is planned to quantify the actual role of the motor and its supports on the fan performance. Another investigation is to considerably reduce the number of volume elements in the calculation domain, applying periodicity conditions, in order to check the accuracy of the prediction. If the results are not too degraded that would significantly reduce the calculation time and/or the number of parallel processors.

REFERENCES

[1] Official Journal of the European Union: Commission Regulation (EU) No 327/2011 implementing Directive 2009/125/EC with regard to ecodesign requirements for fans driven by motors with an electric input power between 125 W and 500 kW, March **2011**.

[2] ISO 5801: *Industrial fans – Performance testing using standardized airways*, **2007**.

[3] ISO 12759: *Fans – Efficiency classification for fans*, **2010**.